Formation of Cubic *Ia*3*d* Silicas and Metal Oxide-Loaded Silicas Using a Triblock Copolymer ($EO_{20}PO_{70}EO_{20}$)−Acetate Mixture as Structure Director in Aqueous Solution

Zheng Ying Wu, Yi Meng Wang, Wan Wei Huang, Jing Yang, Hong Ji Wang, Jia Hui Xu, Yi Lun Wei, and Jian Hua Zhu*

Key Laboratory of Mesoscopic Chemistry, School of Chemistry and Chemical Engineering, Nanjing University, Nanjing 210093, China

Received October 3, 2006. Revised Manuscript Received January 4, 2007

Mesoporous silica with *Ia*3*d* structure has been successfully prepared utilizing a triblock copolymer ($EO_{20}PO_{70}EO_{20}$)−acetate mixture for structure direction in aqueous solution over a wide pH range, even above the isoelectric point of silica, where the pH value could be finely tuned by varying the concentration of HCl and/or acetate. Characterization by XRD, TEM, and N_2 sorption measurements show that the cubic *Ia*3*d* materials possess high surface areas (about 900 m^2/g), large pore volumes (about 1.2 cm^3/g), and uniform pore diameters (about 9.2 nm). Further, the phase diagram in the SiO_2−P123−$ZnAc_2$−H_2O−HCl system is drawn to map the range of cubic mesophase. Salt effect has been investigated during the phase transformation process, which reveals that the nature and concentration of cations can also determine the mesostructure. In addition, when two different acetates are introduced into the solution at one time, metal oxides-modified cubic mesoporous silica can be directly synthesized. Among others, copper-modified cubic samples, prepared by this direct method, display superior properties in the NO_2-TPD experiments. The lower acid concentration in the acetate-modulated synthetic system favors the direct incorporation of metal oxide species and this discovery may offer us a new perspective to better understand the formation mechanism of ordered mesoporous materials.

Introduction

Mesoporous material such as M41S, since its initial report in 1992,[1,2] has greatly inspired research interests in various fields including catalysis, adsorption, separation, sensing, drug delivery, optoelectronics, and the manufacture of advanced nanostructured materials.[3−5] Among these novel materials, the phases with a three-dimensional pore system are believed to be more advantageous for catalytic applications than those phases having a one-dimensional array of pores.[6] Particularly, mesoporous MCM-48 material with the 3-D cubic *Ia*3*d* mesostructure possessing a bicontinuous structure centered on the gyroid minimal surface that divides available pore space into two nonintersecting subvolumes attracts more attention.[7] With the high specific surface area, pore volume, and high thermal stability, MCM-48 materials are widely used as adsorbents and catalyst supports in separation techniques or catalytic reactions. The reason why MCM-48 seems to be more interesting than MCM-41 relies on its interwoven and branched pore structure, which provides more favorable mass-transfer kinetics in catalytic and separation applications than MCM-41 with its unidirectional pore system.[8] In total, the open pore structure of MCM-48 offers the more easy and direct access for guest species, thus facilitating inclusion or diffusion throughout the pore channels without pore blockage.[9] However, fewer investigations have been reported on the cubic 3-D mesoporous MCM-48 than on MCM-41[10] because of the small domain of this cubic phase (*Ia*3*d*) of MCM-48 in phase diagrams and the more restricted synthesis condition.[11] Therefore, exploiting a facile synthetic way of preparing 3-D cubic *Ia*3*d* mesoporous silicas is attractive for many researchers.

MCM-48 with cubic *Ia*3*d* symmetry is traditionally synthesized with cationic alkylammonium as the surfactant under alkaline conditions in a narrow range of compositions and quite high temperatures.[12] Subsequently, using cationic surfactant, either mixed cationic−anionic or cationic−neutral

* To whom correspondence should be addressed. E-mail: jhzhu@netra.nju.edu.cn. Fax: +86-25-83317761. Tel.: +86-25-83595848.

(1) Kresge, C. T.; Leonowicz, M. E.; Roth, W. J.; Vartuli, J. C.; Beck, J. C. *Nature* **1992**, *359*, 710.
(2) Beck, J. S.; Vartuli, J. C.; Roth, W. J.; Leonowicz, M. E.; Kresge, C. T.; Schmitt, K. D.; Chu, C. T. W.; Olson, D. H.; Sheppard, E. W.; Mac Cullen, S. B.; Higgins, J. B.; Schlenker, J. L. *J. Am. Chem. Soc.* **1992**, *114*, 10834.
(3) Scott, B. J.; Wirnsberger, G.; Stucky, G. D. *Chem. Mater.* **2001**, *13*, 3140.
(4) Stein, A. *Adv. Mater.* **2003**, *15*, 763.
(5) Taguchi, A.; Schüth, F. *Microporous Mesoporous Mater.* **2004**, *77*, 1.
(6) Vinu, A.; Krithiga, T.; Balasubramanian, V. V.; Asthana, A.; Srinivasu, P.; Mori, T.; Ariga, K.; Ramanath, G.; Ganesan, P. G. *J. Phys. Chem. B* **2006**, *110*, 11924.
(7) Schumacher, K.; Ravikovitch, P. I.; Chesne, A. D.; Neimark, A. V.; Unger, K. K. *Langmuir* **2000**, *16*, 4648.
(8) Schumacher, K.; Grun, M.; Unger, K. K. *Microporous Mesoporous Mater.* **1999**, *27*, 201.
(9) Rolison, D. R. *Science* **2003**, *299*, 1698.
(10) Flodström, K.; Alfredsson, V.; Källrot, N. *J. Am. Chem. Soc.* **2003**, *125*, 4402.
(11) Liu, X. Y.; Tian, B. Z.; Yu, C. Z.; Gao, F.; Xie, S. H.; Tu, B.; Che, R. C.; Peng, L. M.; Zhao, D. Y. *Angew. Chem., Int. Ed.* **2002**, *41*, 3876.
(12) Morey, M. S.; Davidson, A.; Stucky, G. D. *J. Porous Mater.* **1998**, *5*, 195.

10.1021/cm0623615 CCC: $37.00
Published on Web 02/28/2007

surfactant, as structure-directing agent is developed.[13,14] Later, cubic *Ia*3*d* mesoporous silicas are obtained under acidic conditions by utilizing the laboratory-synthesized cationic surfactant cetyltriethylammonium bromide (CTEABr), and the low temperature of 273 K is needed during the reaction.[15,16] However, all of these cubic *Ia*3*d* MCM-48-type mesoporous materials have relatively small pore sizes (usually below 4 nm), which is unfavorable for the applications dealing with large molecules, and very often the small framework wall thickness leading to poor thermal and hydrothermal stability. Therefore, large-pore cubic *Ia*3*d* mesoporous silicas with more stability are in demand. Using block copolymer as structure-directing agent seems to be a nice method.[17−25] When commercially available triblock copolymers Pluronic P123 is employed as structure-directing agent, however, some additives such as trialkoxyorganosilane including triethoxyvinylsilane and 3-mercaptopropyltrimethoxysilane,[18,19] NaI salt,[20] butanol,[21] or anionic sodium dodecyl sulfate (SDS)[22] must be added; otherwise, no *Ia*3*d* mesostructures form. Cubic *Ia*3*d* monolithic silica (HOM-5) has even been synthesized by using instantly preformed liquid-crystalline phases of surfactant in bulk lyotropic and microemulsion systems,[24,25] but this hard, translucent, and crack-free material has different properties from the traditional hydrothermal prepared powder materials. Recently, Ryoo and co-workers greatly extended the phase domain for the cubic *Ia*3*d* mesoporous silica, whereas the amounts of acid, BuOH, and silica source were changed correspondingly and allowed facile syntheses.[21c] However, these block copolymer-templated *Ia*3*d* mesoporous silicas are still synthesized under strong acidic conditions (well below the isoelectric point of silica).

Low acid concentrations favor not only the facile preparation of high-quality mesoporous silicas using block copolymers[26] but also the direct incorporation of metal cations into the framework of mesoporous materials under acidic conditions.[27] As we know, metal- or metal oxide-loaded cubic materials are widely investigated by many researchers.[8,28−33] However, few papers have been reported on the direct incorporation of metal sites on cubic material under decreased acidic conditions except for the example of cubic FeSBA-16,[34] for the synthetic domain of the cubic phase is always narrower than that of the hexagonal phase and decreasing the acid concentration easily led to disordered mesostructure. In the preparation of FeSBA-1, Fe species could be incorporated into SBA-1 by simply adjusting the molar hydrochloric acid-to-silicon ratio in the synthesis gel but this synthesis should be taken under very low temperature of 273 K and the amount of incorporated Fe seemed limited.[34] Here, we report the synthesis of large-pore cubic *Ia*3*d* mesoporous silicas directly from the synthetic system similar to that of SBA-15 with the assistance of acetate. After introduction of several acetate salts into the solution consisting of commercial P123 copolymer and HCl, the pH value could be tuned above and below the isoelectric point of silica (pH = 2) and then cubic structure could be obtained over a wider pH range. Further, the synthesis could be carried at different temperatures from 288 to 313 K with another hydrothermal treatment step utilizing different bivalent cations. This method also provides many possibilities of incorporating a large amount of metal oxide species into the cubic mesoporous material without the loss of *Ia*3*d* symmetry. More than 20 wt % copper could be directly incorporated into the cubic material and the modified cubic silicas show superior adsorptive properties in NO_2-TPD experiments.

Experimental Section

The large-pore cubic mesoporous silica with *Ia*3*d* symmetry was prepared by the following procedure that is similar to the method of synthesizing traditional SBA-15[35] except for introduction of several salts. Apart from the use of the triblock poly(ethylene oxide)−poly(propylene oxide)−poly(ethylene oxide) copolymer Pluronic P123 ($EO_{20}PO_{70}EO_{20}$, M_{av} = 5800) and tetraethyl orthosilcate (TEOS), many salts of bivalent cation including $Zn(CH_3COO)_2$, $Mg(CH_3COO)_2$, $Ca(CH_3COO)_2$, $Cu(CH_3COO)_2$, and $Mg(NO_3)_2$ were employed. In a typical synthesis, 2 g of Pluronic P123 and a calculated amount of salt were dissolved in 15 g of H_2O and 60 g of 2 M HCl to achieve a clear solution. Thereafter, 4.25 g of TEOS was added under stirring at a given temperature (288−313 K). The molar composition of the mixture was 1:0.017:*x*:6:192 TEOS:P123:salt:HCl:H_2O, and all the mixtures were maintained under stirring

(13) (a) Chen, F.; Huang, L.; Li, Q. *Chem. Mater.* **1997**, *9*, 2685. (b) Chen, F.; Song, F.; Li, Q. *Microporous Mesoporous Mater.* **1999**, *29*, 305. (c) Zhao, W.; Li, Q. Z. *Chem. Mater.* **2003**, *15*, 4160.
(14) (a) Ryoo, R.; Joo, S. H.; Kim, J. M. *J. Phys. Chem. B* **1999**, *103*, 7435. (b) Kruk, M.; Jaroniec, M.; Ryoo, R.; Joo, S. H. *Chem. Mater.* **2000**, *12*, 1414.
(15) Che, S.; Lim, S.; Kaneda, M.; Yoshitake, H.; Terasaki, O.; Tatsumi, T. *J. Am. Chem. Soc.* **2002**, *124*, 13962.
(16) Ogura, M.; Miyoshi, H.; Naik, S. P.; Okubo, T. J. *Am. Chem. Soc.* **2004**, *126*, 10937.
(17) Chan, Y. T.; Lin, H. P.; Mou, C. Y.; Liu, S. T. *Chem. Commun.* **2002**, 2878.
(18) Hodgkins, R. P.; Garcia-Bennett, A. E.; Wright, P. A. *Microporous Mesoporous Mater.* **2005**, *79*, 241.
(19) Wang, Y. Q.; Yang, C. M.; Zibrowius, B.; Spliethoff, B.; Lindén, M.; Schüth, F. *Chem. Mater.* **2003**, *15*, 5029.
(20) Flodstrom, K.; Wennerstrom, H.; Teixeira, C. V.; Amenitsch, H.; Linden, M.; Alfredsson, V. *Langmuir* **2004**, *20*, 10311.
(21) (a) Kleitz, F.; Choi, S. H.; Ryoo, R. *Chem. Commun.* **2003**, 2136. (b) Sakamoto, Y.; Kim, T.-W.; Ryoo, R.; Terasaki, O. *Angew. Chem., Int. Ed.* **2004**, *43*, 5231. (c) Kim, T.-W.; Kleitz, F.; Paul, B.; Ryoo, R. *J. Am. Chem. Soc.* **2005**, *127*, 7601.
(22) Chen, D.; Li, Z.; Yu, C.; Shi, Y.; Zhang, Z.; Tu, B.; Zhao, D. Y. *Chem. Mater.* **2005**, *17*, 3228.
(23) Chen, D.; Li, Z.; Wan, Y.; Tu, X.; Shi, Y.; Chen, Z.; Shen, W.; Yu, C.; Tu, B.; Zhao, D. *J. Mater. Chem.* **2006**, *16*, 1511.
(24) El-Safty, S. A.; Hanaoka, T. *Adv. Mater.* **2003**, *15*, 1893.
(25) El-Safty, S. A.; Hanaoka, T.; Mizukami, F. *Adv. Mater.* **2005**, *17*, 47.
(26) (a) Choi, M.; Heo, W.; Kleitz, F.; Ryoo, R. *Chem. Commun.* **2003**, 1340. (b) Kleitz, F.; Liu, D.; Anilkumar, G. M.; Park, I. S.; Solovyov, L. A.; Shmakov, A. N.; Ryoo, R. *J. Phys. Chem. B* **2003**, *107*, 14296.
(27) (a) Vinu, A.; Murugesan, V.; Bohlmann, W.; Hartmann, M. *J. Phys. Chem. B* **2004**, *108*, 11496. (b) Vinu, A.; Sawant, D. P.; Ariga, K.; Hossain, K. Z.; Halligudi, S. B.; Hartmann, M.; Nomura, M. *Chem. Mater.* **2005**, *17*, 5339. (c) Vinu, A.; Srinivasu, P.; Miyahara, M.; Ariga, K. *J. Phys. Chem. B* **2006**, *110*, 801.
(28) Koo, D. H.; Kim, M.; Chang, S. *Org. Lett.* **2005**, *7*, 5015.
(29) Guo, X.-J.; Yang, C.-M.; Liu, P.-H; Cheng, M.-H.; Chao, K.-J. *Cryst. Growth Des.* **2005**, *5*, 33.
(30) Kustrowski, P.; Chmielarz, L.; Dziembaj, R.; Cool, P.; Vansant, E. F. *J. Phys. Chem. B* **2005**, *109*, 11552.
(31) Echchahed, B.; Moen, A.; Nicholson, D.; Bonneviot, L. *Chem. Mater.* **1997**, *9*, 1716.
(32) Hartmann, M.; Racouchot, S.; Bischof, C. *Chem. Commun*. **1997**, 2367.
(33) Pantazis, C. C.; Trikalitis, P. N.; Pomonis, P. J. *J. Phys. Chem. B* **2005**, *109*, 12574.
(34) Vinu, A.; Krithiga, T.; Murugesan, V.; Hartmann, M. *Adv. Mater.* **2004**, *16*, 1817.
(35) Zhao, D. Y.; Feng, J. L.; Huo, Q. S.; Melosh, N.; Fredrickson, G. H.; Chmelka, B. F.; Stucky, G. D. *Science* **1998**, *279*, 548.

at a given temperature for 24 h and then heated at 373 K for another 24 h under static conditions. The products were filtered and washed with water, and the polymer was removed by calcination in air at 773 K for 5 h. To assess the distribution of copper deposited on cubic *Ia*3*d* sample, 0.2 g of the as-synthesized composite was added into 2 g of 10 wt % NaCl solution, then stirred for 24 h to exchange ion,[36] and filtrated, dried, and calcined prior to detecting copper and sodium content.

X-ray diffraction (XRD) patterns were recorded on an ARL XTRA diffractometer with Cu Kα radiation in the 2θ ranges from 0.5 to 5° or from 5 to 80°. TEM analysis was performed on a FEI Tecnai G2 20 S-TWIN electron microscope operating at 200 kV, and a Micromeritics ASAP 2020 instrument utilized for measuring the nitrogen adsorption−desorption isotherms at 77 K where the siliceous samples were evacuated at 573 K and the copper-modified ones evacuated at 423 K for 4 h in the degas port. The Brunauer−Emmett−Teller (BET) specific surface areas of the samples were calculated using adsorption data in the relative pressure range from 0.04 to 0.2, and the total pore volumes were determined from the amount adsorbed at a relative pressure of about 0.99. The pore size distribution (PSDs) curves were calculated from the analysis of the adsorption branch of the isotherm, using the Barret−Joyner−Halenda (BJH) algorithm. The pH value was measured by use of a pH meter with model of PHS-3C, while the copper contents of the copper-modified samples were measured by inductive coupled plasma-atomic emission spectrometry (ICP-AES). X-ray photoelectron spectra (XPS) measurements were performed on the instrument of Thermo ESCALAB 250 using Al Kα radiation (1486.6 eV), and C 1s (284.6 eV) was utilized as a reference to correct the binding energy. UV−vis diffraction reflection (DR) spectra were recorded on a UV-2401 (Shimadzu) spectrophotometer adapted with a praying mantis accessory using $BaSO_4$ as a standard. FTIR test was performed on a set of BRUKER 22 FTIR spectrometer with the tablet of samples and KBr. NO_2-TPD experiments were carried out as reported previously;[37] 0.1 g of sample was placed in a glass microreactor and activated in N_2 at 773 K for 2 h and then cooled to 313 K prior to contacting 0.320 mmol of NO_2. After the adsorbent was purged for 1 h by the carrier gas to remove the physically adsorbed NO_2, it was heated to 773 K at a rate of 10 K/min; meanwhile, the released NO_2 was detected by colorimetric method.[38]

Results

(A) Formation of *Ia*3*d* Mesostructured Silica by Adding Zinc Acetate. Figure 1A depicts the XRD patterns of the as-synthesized mesoporous materials prepared by adding different amounts of zinc acetate in the synthetic system at 308 K. In the case of $x = 1$ and $x = 2$ (x denoted as the molar ratio of $Zn(CH_3COO)_2$/TEOS), the products exhibit the typical XRD patterns of the two-dimensional hexagonal pore ordering of *p*6*mm* symmetry, identical to that of SBA-15. When $x = 3$, the mesostructure of the product begins deviating from a typical *p*6*mm* symmetry. A new diffraction peak at 2θ of 1.08° emerges near the main peak at 2θ of 0.96°, while the two peaks of (110) and (200) according to *p*6*mm* symmetry are weakened and distorted, which suggests the presence of some intermediate mixed phases between

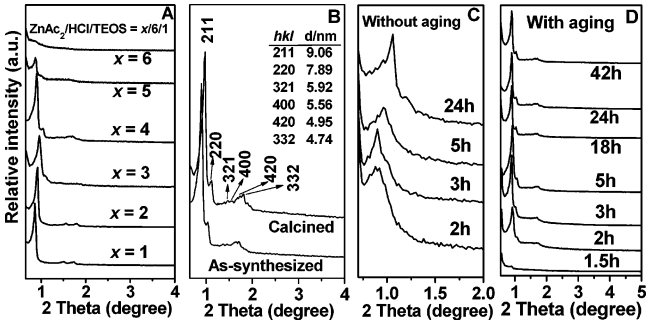

Figure 1. XRD patterns of the as-synthesized samples (A) synthesized with the molar ratio of $Zn(CH_3COO)_2$/HCl/TEOS = x/6/1, x varied from 1 to 6; (B) the as-prepared and calcined sample synthesized with the molar ratio of $Zn(CH_3COO)_2$/HCl/TEOS = 4/6/1; (C) the sample synthesized with the molar ratio of $Zn(CH_3COO)_2$/HCl/TEOS = 4/6/1 stirring at 308 K for different lengths of time; (D) the sample synthesized with the molar ratio of $Zn(CH_3COO)_2$/HCl/TEOS = 4/6/1 stirring at 308 K for different lengths of time and then aging at 373 K for 24 h.

*p*6*mm* and *Ia*3*d* symmetry. With further enhancement of the concentration of zinc acetate to $x = 4$, a mesophase with the bicontinuous cubic *Ia*3*d* space group is formed. Six well-resolved diffraction peaks indexed to (211), (220), (321), (400), (420), and (332) reflections of the bicontinuous cubic *Ia*3*d* structure are clearly observed in the XRD patterns (Figure 1B), indicating the formation of the highly ordered cubic material with a three-dimensional *Ia*3*d* symmetry. The mesostructure of the sample is maintained after calcination at 773 K in air, implying its high thermal stability. The unit cell parameter, a, calculated from the (211) reflection of the as-synthesized or calcined cubic sample, is 24.1 or 22.2 nm, respectively. This value is much larger than that of the tetraalkylammonium-based cubic analogues such as MCM-48, as triblock polymer P123 templated materials always have large pore size.[19,22] Further increasing the amount of zinc acetate will lead to less ordered or disordered structure. The ordering of the cubic *Ia*3*d* mesostructure obviously decreases as the value of x achieves 5 and disordered mesostructure emerges when x reaches 6, which suggests that highly ordered bicontinuous cubic *Ia*3*d* mesostructure only can be prepared with the appropriate zinc acetate concentration of $x = 4$ in the case of keeping the concentration of other composites unchangeable ($Zn(CH_3COO)_2$/HCl/TEOS = x/6/1). Hydrothermal aging process is an important step for the synthesis of cubic *Ia*3*d* sample, whose impact is revealed in Figures 1C and 1D where the XRD patterns of these samples synthesized with or without aging are depicted. It is clear that mesophase is formed after stirring the synthetic solution for 2 h and maintained with prolonged stirring time. Figure 1C shows that cubic structure with *Ia*3*d* symmetry appears in the case of stirring the mixture for 24 h but the mesostructure is not very ordered without aging. Hydrothermal treatment is very valuable to improve the ordering of the mesostructure. When the starting mixture was stirred for 2 h and further heated at 373 K for 24 h, more ordered sample could be gained. Likewise, highly ordered mesostructure with *Ia*3*d* symmetry can be obtained if the mixture was stirred for 3 h and then aged at 373 K. Prolonging the stirring time from 3 to 42 h and then hydrothermally treating the samples show no obvious improvement for the mesostructure of the cubic samples.

(36) Varga, J.; Nagy, J. B.; Halisz, J.; Kiricsi, I. *J. Mol. Struct.* **1997**, *410*−*411*, 149.
(37) Xu, Y.; Zhu, J. H.; Ma, L. L.; Ji, A.; Wei, Y. L.; Shang, X. Y. *Microporous Mesoporous Mater.* **2003**, *60*, 125.
(38) Saltzman, B. E. *Anal. Chem.* **1954**, *26*, 1949.

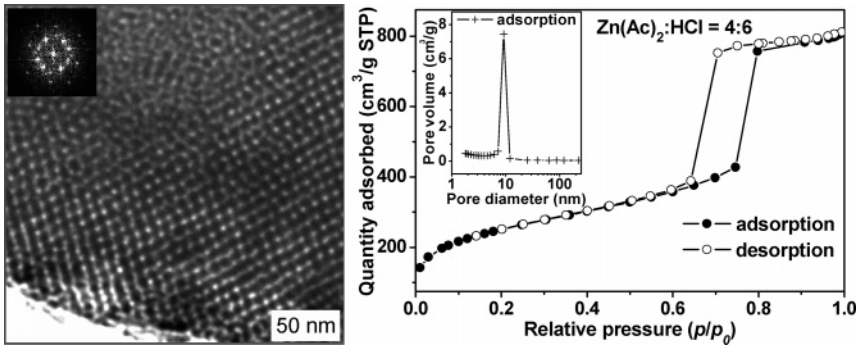

Figure 2. (left) TEM image recorded along the [531]-direction and (right) N_2 adsorption−desorption isotherm (the inset is pore size distribution) of the calcined cubic *Ia*3*d* mesoporous silica prepared with $Zn(CH_3COO)_2$/HCl/TEOS = 4/6/1 at 308 K.

Table 1. Physical Properties of the *Ia*3*d* Structured Mesoporous Silica

sample[a]	T[b] (K)	pH value	a_0 (nm)	S_{BET} (m^2/g)	S_{mic} (m^2/g)	V_p (cm^3/g)	V_{mic} (cm^3/g)	D_p (nm)
$Zn(CH_3COO)_2$/Si = 4/1	308	3.07	22.2	903	167	1.23	0.07	9.2
$Mg(CH_3COO)_2$/Si = 3/1	288	1.02	23.5	820	57	1.31	0.06	9.5
$Ca(CH_3COO)_2$/Si = 3/1	288	2.58	20.4	1021	123	1.49	0.04	9.0
$Cu(CH_3COO)_2$/Si = 3/1	308	1.01	21.6	809	228	0.75	0.10	7.4
$Mg(NO_3)_2$/Si = 4/1	313	c	21.2	773	156	1.01	0.06	7.5

[a] The molar composition of the mixtures is TEOS/P123/salt/HCl/H_2O = 1/0.017/*x*/6/192. [b] This temperature refers to that of the first step under stirring. [c] The mixture is strong acidic with $[H^+] > 1$ M.

The exact assignment of the sample synthesized with the molar composition of $Zn(CH_3COO)_2$/HCl/TEOS = 4/6/1 to the *Ia*3*d* symmetry is confirmed by transmission electron microscopy. Cubic mesostructure can be observed in the TEM image, as shown in Figure 2A. The unit cell size of calcined sample obtained from TEM analysis is 20.1 nm, coincided with that calculated from XRD measurement. This calcined mesoporous *Ia*3*d* silica possesses the nitrogen adsorption−desorption isotherm of type IV with a sharp capillary condensation step at high relative pressures (p/p_0 = 0.7−0.8), along with an H_1-type hysteresis loop, indicative of large channel-like pores in a narrow range of size, as shown in Figure 2. This material synthesized from zinc acetate at 308 K has BET surface area and pore volume of 903 m^2/g and 1.23 cm^3/g, respectively. Furthermore, a narrow pore size distribution with the primary value of 9.2 nm is calculated from the adsorption branch by the BJH method (Table 1).

As mentioned above, cubic mesoporous material with *Ia*3*d* symmetry can be gained if zinc acetate is introduced into the synthetic mixture containing P123 and HCl. However, in this system the molar ratio of HCl/TEOS should be fixed to 6/1, and highly ordered cubic samples are gained only with high zinc acetate concentration ($Zn(CH_3COO)_2$/HCl/TEOS = 4/6/1). To explore whether the highly ordered sample can be prepared with the varied concentration of HCl and zinc acetate, the influence of the amount of zinc acetate and HCl is studied. Figure 3 illustrates the XRD patterns of the as-synthesized samples prepared under different molar compositions of $Zn(CH_3COO)_2$/HCl and pH values of all of the batch were also detected (Figure S1). Only 2-D hexagonal phase is formed when $x = 1$ (*x*/*y*/1 $Zn(CH_3COO)_2$/HCl/TEOS) no matter how the molar rato of HCl varied from 1 to 6 (Figure 3A). No cubic *Ia*3*d* structure formed under the low zinc acetate concentration, which suggests that the salt effect may be too weak to lead to a phase transformation from *p*6*mm* to *Ia*3*d*. Nevertheless, mesophase transition

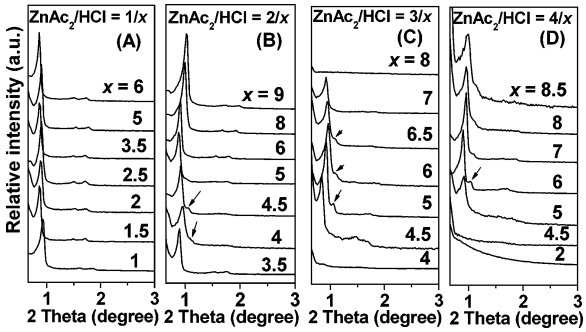

Figure 3. XRD patterns of the as-synthesized samples synthesized with different molar ratios of *x*/*y*/1 $Zn(CH_3COO)_2$/HCl/TEOS.

occurs if increasing the zinc acetate to $x = 2$ while the HCl concentration varies simultaneously. At $x = 2$, phase transformation occurs when *y* is tuned up from 3.5 to 4, and well-developed cubic *Ia*3*d* mesophase (d_{211} = 9.6 nm) is achieved if the molar ratio of HCl/TEOS (*y*) increases to 4.5. When the molar ratio of HCl/TEOS (*y*) is raised to 5 or more, hexagonal mesophase like conventional SBA-15 emerges (Figure 3B). Hence, there must be some correlations between the amount of zinc acetate and HCl. In another words, phase transformation from *p*6*mm* to *Ia*3*d* will take place if the molar ratios of *x*/*y*/1 $Zn(CH_3COO)_2$/HCl/TEOS are suitable. In the case of $x = 3$, phase transformation is not well-developed and then some intermediate phases are acquired at $y = 4.5$, whereas the highly ordered cubic *Ia*3*d* material (d_{211} = 9.6 nm) is obtained at $y = 5$. The ordering of cubic *Ia*3*d* silicas decreases with a further increase in *y* ratio, as shown in Figure 3C; finally, a disordered sample is attained at $y = 8$. When $x = 4$, highly ordered cubic *Ia*3*d* material is procured at $y = 6$, and less-ordered samples are gained at $y = 7$, 8, and 8.5. It should be pointed out that, at the high concentration of zinc acetate with $x = 3$ and 4, the ordered mesostructures including both hexagonal and cubic symmetry can be obtained in the range of $4 < y < 9$ (pH value varied from 0.4 to 3.4), which is different from the

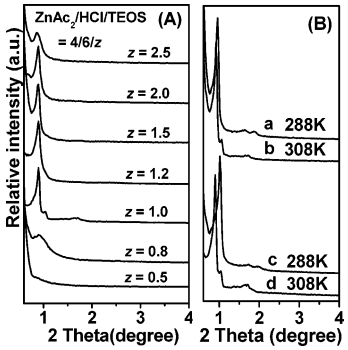

Figure 4. XRD patterns of the as-synthesized (A) samples synthesized with different amounts of TEOS: the molar ratio of the sample is 4/6/*z* $Zn(CH_3COO)_2$/HCl/TEOS, *z* varied from 0.5 to 2.5; (B) samples synthesized with different temperatures: (a) and (b) $Zn(CH_3COO)_2$/HCl/TEOS = 3/5/1; (c) and (d) $Zn(CH_3COO)_2$/HCl/TEOS = 4/6/1.

system with relatively low concentration of zinc acetate. We think the acidity and the salt concentrations of the solution may play important roles in the phase formation during the synthesis.

Figure 4A displays the influence of TEOS amount in the initial reaction mixture on the structure of synthetic products, especially in the case that the molar ratio of zinc acetate to HCl is fixed to 4/6 (4/6/*z* $Zn(CH_3COO)_2$/HCl/TEOS); meanwhile, the amount of TEOS varies from $z = 0.5$ to $z = 2.5$. Disordered sample is obtained in the synthesis with low TEOS concentration ($z = 0.5$); less-ordered phase appears at $z = 0.8$ while highly ordered cubic structure emerges once *z* value achieves 1.0. Further increase in the amount of TEOS to $z = 1.2$, 1.5, and 2.0 weakens the peak identical to (220) reflections of cubic *Ia*3*d* structure; meanwhile, the pseudo-cubic samples appear as shown in Figure 4A. Less-ordered structure forms when the *z* value reaches 2.5, indicating that overfull TEOS is not beneficial for forming the ordered cubic phase. Further, no ordered structure can be gained at $z = 0.5$ no matter how the molar ratio of zinc acetate to HCl varies (*x*/*y*/0.5 $Zn(CH_3COO)_2$/HCl/TEOS) (Figure S2A). Likewise, various structures can be formed in the case that the molar ratio of Zn/Si is fixed to 4/0.8 while the amount of HCl varies (4/*y*/0.8 $Zn(CH_3COO)_2$/HCl/TEOS). Disordered or less-ordered structures are observed when $y = 5.5$ or 6.0, as shown in Figure S2B. In contrast, ordered cubic sample can be attained if the amount of HCl rose to $y = 6.5$ and 7.0, as if the acidity played a role similar to that of the silica source such as TEOS.

Figure 4 also shows the XRD patterns to indicate the influence of reaction temperature. Only hexagonal *p*6*mm* silica is obtained at 288 K in the system with the molar composition of $Zn(CH_3COO)_2$/HCl/TEOS = 3/5/1 and 4/6/1, while cubic *Ia*3*d* materials form at 308 K. In the situation that phase transformation occurs during the drying process, drying at a higher temperature will promote the phase transformation of hexagonal to cubic because the conformational disorder of the surfactant tail is enhanced, increasing the effective molecular volume and causing a corresponding increase in the *g* value.[16] However, less ordered structure is earned in the sample synthesized with the molar ratio of Zn-$(CH_3COO)_2$/HCl/TEOS = 4/6/1 when reaction temperature increases to 333 K, indicating that the overheated hydrothermal surroundings are not suitable for the formation of

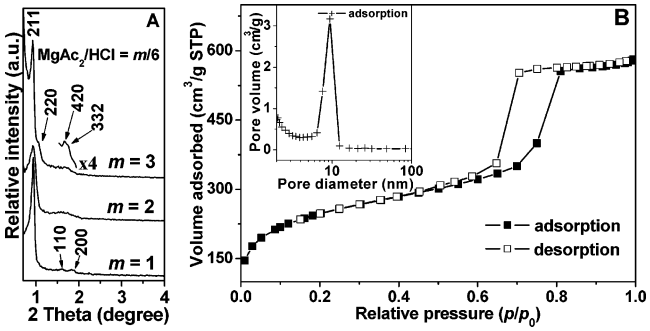

Figure 5. (A) Low-angle XRD patterns of the as-prepared samples synthesized at 288 K with the molar ratio of $Mg(CH_3COO)_2$/HCl/TEOS = *m*/6/1, *m* varied from 1 to 3; (B) N_2 adsorption−desorption isotherm (inset is the pore size distribution) of the calcined cubic *Ia*3*d* mesoporous silica prepared with $Mg(CH_3COO)_2$/HCl/TEOS = 3/6/1 at 288 K.

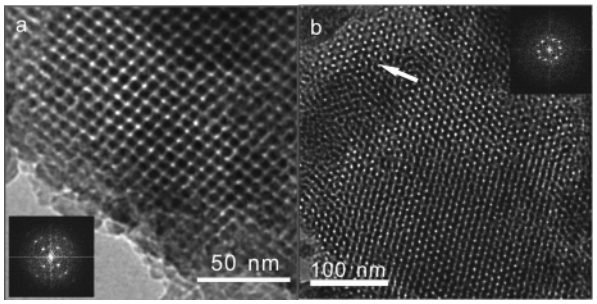

Figure 6. Transmission electron micrographs of the calcined cubic silica synthesized with $Mg(CH_3COO)_2$/HCl/TEOS = 3/6/1 at 288 K. (a) Micrograph recorded along the [100]-direction and (b) micrograph recorded along the [111]-direction for the upper left domain. The corresponding Fourier transforms are inserted.

cubic *Ia*3*d* mesophase. In this zinc acetate-induced system, a mild temperature of 308 K offered a proper situation for the formation of cubic *Ia*3*d* materials.

(B) Formation of *Ia*3*d* Mesostructured Silica by Adding Magnesium Acetate and Other Salts. Zinc acetate is not the unique salt additive to spur the phase transformation in the synthetic solution containing P123 and HCl; adding other acetates such as magnesium, cupric, and calcium salts also leads to the formation of cubic *Ia*3*d* mesostructure provided the temperature and the chemical molar composition of the reaction mixture are suitable. In the case of magnesium acetate, ordered mesoporous materials can be prepared at 288 K and the final mesostructure also can be controlled by the amount of salt added, as shown in Figure 5A. When $m = 1$ (*m* denoted as the molar ratio of $Mg(CH_3COO)_2$/TEOS), the product exhibits the typical XRD pattern of the two-dimensional hexagonal pore ordering of *p*6*mm* symmetry, identical to that of SBA-15. As *m* rises to 2, the mesostructure of the product begins deviating from typical *p*6*mm* symmetry. When *m* reaches 3, a three-dimensional cubic *Ia*3*d* mesophase is obtained, as confirmed by transmission electron micrographs along different directions (Figure 6). In the case of $m = 4$, no ordered mesophase forms.

This as-prepared product with cubic *Ia*3*d* mesostructure synthesized with $Mg(CH_3COO)_2$/HCl/TEOS = 3/6/1 has a lattice parameter of 23.52 nm, and the calcined product possesses the almost same lattice parameter whereas the intensity of diffraction peak increased (Figure S3A). That means, there is no unit cell contraction or silanol group condensation upon the calcination of magnesium-induced

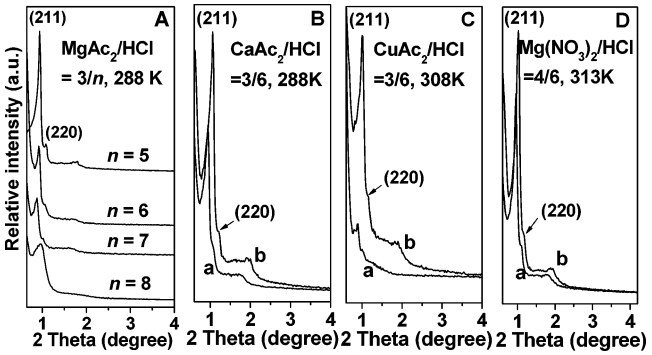

Figure 7. Low-angle XRD patterns of (A) the as-prepared samples synthesized at 288 K with the molar ratio of $Mg(CH_3COO)_2$/HCl/TEOS = 3/*n*/1, *n* varied from 5 to 8; (B), (C), and (D) the as-synthesized (a) and calcined (b) cubic samples prepared by different salts.

samples because a large number of magnesium acetate has been introduced in the synthetic system to improve the condensation of silica.[39] Figure 5B depicts the nitrogen adsorption−desorption isotherm of calcined mesoporous *Ia*3*d* silica. It is type IV with a sharp capillary condensation step at high relative pressures and a H1 hysteresis loop, which is in agreement with that from large-pore cubic *Ia*3*d* mesoporous silica.[22] A narrow pore size with a primary value of 9.5 nm is calculated from the adsorption branch. After calcination, the sample synthesized with magnesium acetate at 288 K has a BET surface area and pore volume of 820 m^2/g and 1.31 cm^3/g, respectively. The relatively small lattice parameter and pore size for SBA-15 synthesized at low temperature can be attributed to salt effect.[40] Here, this cubic *Ia*3*d* silica synthesized with magnesium acetate at 288 K has the comparable lattice parameter and pore size to those synthesized with butanol or NaI additive at high temperature.[20,21] Besides, the amount of KCl used in the synthesis of SBA-15 with a molar ratio KCl/TEOS = 6 at 288 K is much higher than that with $Mg(CH_3COO)_2$/TEOS = 1, which indicates that the bivalent salt may have different influences on the formation of mesoporous materials from KCl and other commonly used additives.

With variation in the amount of HCl in the mixture of 1:0.017:3:*n*:192 TEOS:P123:$Mg(CH_3COO)_2$:HCl:H_2O (molar ratio), the initial pH values of reaction mixtures decrease from 3.2 to 1.0 and 0.3 before the addition of TEOS when $n = 5.1$, 6.0, and 7.0, respectively. All three batches give *Ia*3*d* silica samples but with different lattice parameters. Especially, a highly ordered cubic *Ia*3*d* mesoporous silica is achieved at pH = 3.2 as shown in Figure 7A. In short, these magnesium acetate-induced large-pore cubic *Ia*3*d* silicas are also synthesized both above and below the isoelectric point of silica (pH = 2), the same as the zinc acetate-induced situation. Moreover, the d_{211} spacing of these three samples is 9.4, 9.6, and 10.0 nm, respectively, with $n = 5.1$, 6.0, and 7.0. With further increasing of the HCl concentration up to $n = 8.2$, less ordered mesoporous material is gained. The H^+ concentration in this batch is almost the same as that in the batch of $Mg(CH_3COO)_2$/HCl = 1/6 (pH = −0.19), which demonstrates that the amount of salt still has an important effect in the formation of different mesostructures even at the same pH value.

Other acetates with different bivalent cations or magnesium nitrate can also trigger the formation of cubic *Ia*3*d* mesoporous silica, and the XRD patterns in Figures 7B, 7C, and 7D show the characteristic diffraction peaks of bicontinuous cubic structures in all of the samples. Calcinations of the as-prepared samples lead to lower lattice parameters while the intensity of the characteristic diffraction peak is improved, due to the contractions during the calcinations and enhanced contrasts between silica walls and pore spaces. The lattice parameters are 20.4, 21.6, and 21.2 nm for the samples synthesized by adding calcium acetate, cupric acetate, and magnesium nitrate, respectively (Table 1). The nitrogen adsorption−desorption isotherms of all calcined samples are type IV with a sharp capillary condensation step at relative pressures between 0.60 and 0.80. Narrow pore size distributions of the samples are also observed as shown in Figure 8. Table 1 displays the BET surface areas, pore volumes, and pore sizes of the cubic *Ia*3*d* samples prepared by adding different salts. All of the samples have the large surface areas and pore volumes varied from about 800 to 1000 cm^2/g and 0.75 to 1.49 cm^3/g, respectively.

(C) Direct Incorporation of Metal Oxide Species into Cubic Mesoporous Silica. The cubic masoporous material with *Ia*3*d* symmetry always needs to be functionalized with metal oxides; however, introducing metal oxide into the cubic MCM-48 materials by traditional wetness impregnation often leads to somewhat reduced quality of the symmetry.[41−44] To overcome this problem, a direct synthesis method is developed in our experiments through simultaneously adding zinc acetate and copper acetate into the initial solution, in which both the phase transformation and the deposition of metal salts will happen at the same time at lower H^+ concentration. Figure 9 displays the XRD patterns of the as-prepared copper-modified cubic mesoporous materials synthesized with the addition of both zinc and copper acetates in starting solutions. The cubic materials loaded with different contents of copper oxide will be obtained by the coprecipitation of cupric and siliceous species. Fixing the total molar amount of $Zn(CH_3COO)_2$ and $Cu(CH_3COO)_2$ that were introduced into the synthetic solution to be 4 (*x*/*y*/6/1 $Zn(CH_3COO)_2$/$Cu(CH_3COO)_2$/HCl/TEOS) and then varying the molar composition of Zn^{2+}/Cu^{2+} will lead to different pH value of the solution. Accordingly, different amounts of copper are incorporated into the cubic mesoporous materials. The amount of the deposited copper varies from 0 to 24.2 wt % while the pH value of the solution is altered from 3.0 to 2.4 with the molar ratio of Zn^{2+}/Cu^{2+} changing from 4/0 to 2/2

(39) Wang, Y. M.; Wu, Z. Y.; Wang, H. J.; Zhu, J. H. *Adv. Funct. Mater.* **2006**, *16*, 2374.
(40) Yu, C.; Tian, B.; Fan, J.; Stucky, G. D.; Zhao, D. *Chem. Commun.* **2001**, 2726.
(41) Kumar, D.; Pillai, K. T.; Sudersanan, V.; Dey, G. K.; Gupta, N. M. *Chem. Mater.* **2003**, *15*, 3859.
(42) Bandyopadhyay, M.; Birkner, A.; van den Berg, M. W. E.; Klementiev, K. V.; Schmidt, W.; Grunert, W.; Gies, H. *Chem. Mater.* **2005**, *17*, 3820.
(43) Tkachenko, O. P.; Klementiev, K. V.; Loffler, E.; Ritzkopf, I.; Schuth, F.; Bandyopadhyay, M.; Grabowski, S.; Gies, H.; Hagen, V.; Muhler, M.; Lu, L.; Fischer, R. A.; Grunert, W. *Phys. Chem. Chem. Phys.* **2003**, *5*, 4325.
(44) Gies, H.; Grabowski, S.; Bandyopadhyay, M.; Grunert, W.; Tkachenko, O. P.; Klementiev, K. V.; Birkner, A. *Microporous Mesoporous Mater.* **2003**, *60*, 31.

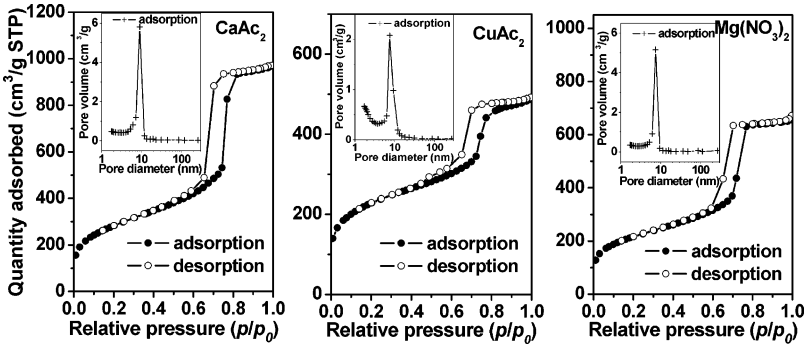

Figure 8. N_2 adsorption−desorption isotherms (the insets are pore size distributions) of the calcined cubic *Ia3d* mesoporous silica prepared with $Ca(CH_3COO)_2$/HCl/TEOS = 3/6/1 at 288 K, $Cu(CH_3COO)_2$/HCl/TEOS = 3/6/1 at 308 K, and $Mg(NO_3)_2$/HCl/TEOS = 4/6/1 at 313 K, respectively.

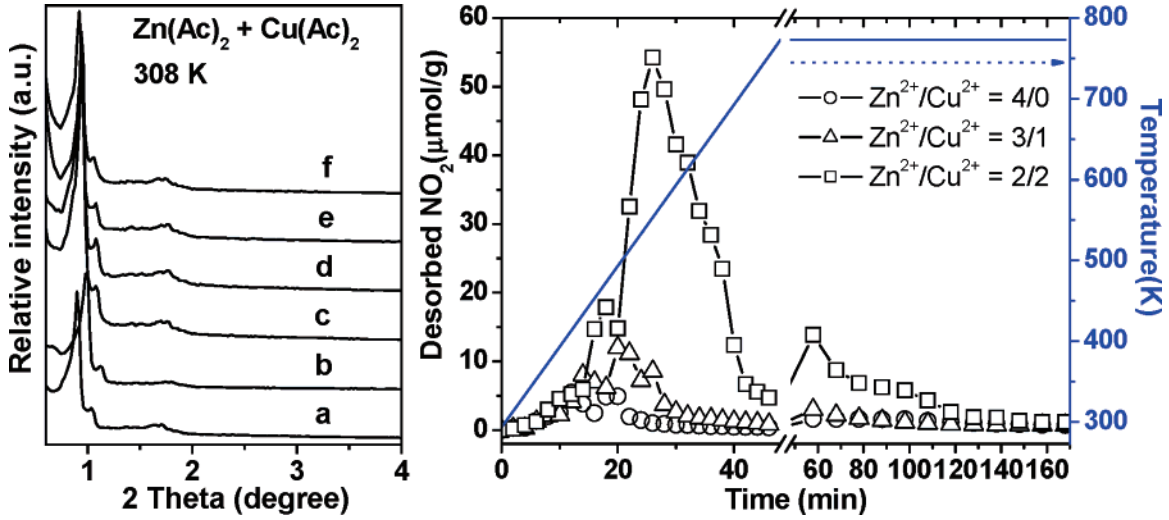

Figure 9. (left) XRD patterns of the as-prepared copper-modified cubic samples with addition of different zinc and cupric acetates in the original solutions. The molar ratio of the sample is *x*/*y*/6/1 $Zn(CH_3COO)_2/Cu(CH_3COO)_2$/HCl/TEOS: (a) Zn^{2+}/Cu^{2+} = 4/0, (b) Zn^{2+}/Cu^{2+} = 3.1/0.9, (c) Zn^{2+}/Cu^{2+} = 3/1, (d) Zn^{2+}/Cu^{2+} = 2.9/1.1, (e) Zn^{2+}/Cu^{2+} = 2.5/1.5, and (f) Zn^{2+}/Cu^{2+} = 2/2; (right) NO_2-TPD of the copper-modified cubic samples.

Table 2. Physical and Catalytic Properties of the CuO-Modified *Ia3d* Structured Mesoporous Silica

sample[a]	Cu (%)	Zn (%)	S_{BET} (m^2/g)	S_{mic} (m^2/g)	V_p (cm^3/g)	V_{mic} (cm^3/g)	D_p (nm)	desorbed NO_2 (μmol/g)	peak (K)
Zn^{2+}/Cu^{2+} = 4/0		0.01	712	133	1.05	0.05	9.2	53	413
Zn^{2+}/Cu^{2+} = 3/1	0.86	0.03	532	22	0.95	0.02	9.2	100	493
Zn^{2+}/Cu^{2+} = 2/2	24.20	0.20	369	26	0.67	0.02	7.6	506	553
Imp24Cu/OMMs[b]	24.20		210	6	0.47	0.01	9.2		

[a] All the samples were degassed at 423 K for 4 h. [b] This sample was prepared by traditional impregnation method.

(Table 2). Meanwhile, all the copper-modified samples are highly ordered with *Ia3d* symmetry, as is evident from the XRD patterns in Figure 9. The *d* values of the copper salts co-directed samples are a bit smaller than that of the sample directed only by zinc acetate. The intensity of the main d_{211} peak first increased and then lightly decreased with the amount of copper acetate increasing. When the copper acetate increases to Zn^{2+}/Cu^{2+} = 3/1, $Cu_2(OH)_3Cl$ crystalline phase emerges in the as-prepared sample and its peak intensity distinctly rises in the sample synthesized with the molar composition of Zn^{2+}/Cu^{2+} = 2/2 (Figure 10A). Since the crystalline $Cu_2(OH)_3Cl$ phase can be transformed to crystalline CuO phase by calcination at 773 K, the crystalline phase of CuO consequently emerges in the calcined sample synthesized with the molar composition of Zn^{2+}/Cu^{2+} = 2.9/1.1, while the peak of CuO is obviously observed in the analogue synthesized with the molar ratio of Zn^{2+}/Cu^{2+} = 2/2 (Figure 10B).

The strange phenomenon in the present investigation that a large amount of copper deposited on the cubic OMMs (ordered mesoporous materials) but only a small amount of zinc remained is amusing, and in our opinion the pH value of the solution is an important factor. It is known that the solubility product constant (K_{sp}) of $Cu(OH)_2$ and $Zn(OH)_2$ are 2.2×10^{-20} and 1.3×10^{-17}, respectively[45] Hence, zinc ion could be precipitated at a pH value larger than 5.8, while copper ion is precipitated as copper hydroxide in the case of pH value larger than 4.5. Therefore, copper ion may deposit on the cubic materials at a lower pH value than zinc ion. However, the pH value of the synthetic solution with a molar composition of P123/HCl/$Zn(CH_3COO)_2$/TEOS = 0.017/6/4/1 is about 3.0, and there seems to be not enough hydroxide ions in the starting solution, leading to the

(45) Dean, J. A. *Lange's Handbook of Chemistry*, 15th ed.; McGraw-Hill Inc.: New York, 1999.

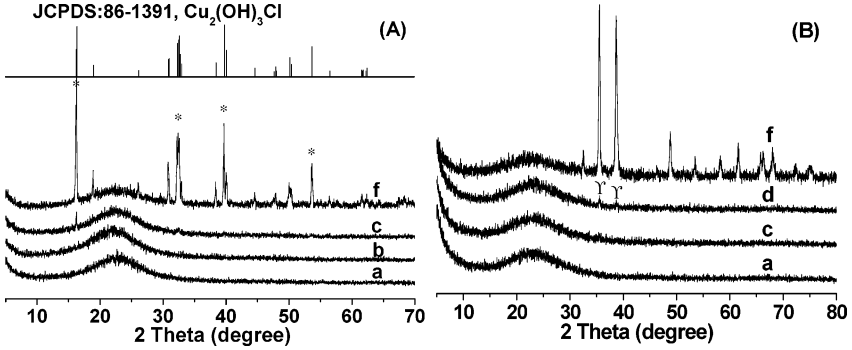

Figure 10. Wide-angle XRD patterns of the as-prepared (A) and calcined (B) copper-modified cubic mesoporous materials with addition of different zinc and copper acetates in original solutions: (a) $Zn^{2+}/Cu^{2+} = 4/0$, (b) $Zn^{2+}/Cu^{2+} = 3.1/0.9$, (c) $Zn^{2+}/Cu^{2+} = 3/1$, (d) $Zn^{2+}/Cu^{2+} = 2.9/1.1$, and (f) $Zn^{2+}/Cu^{2+} = 2/2$.

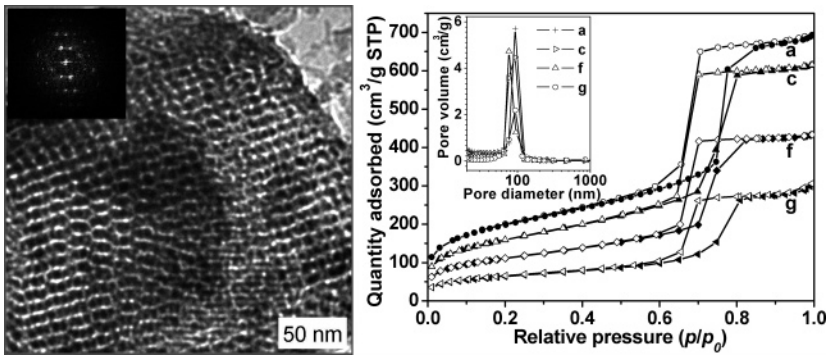

Figure 11. (left) TEM image of the cubic sample synthesized with molar ratio of $Zn^{2+}/Cu^{2+} = 2/2$, view along [311]-direction. (right) N_2 adsorption−desorption isotherms (the insets are pore size distributions) of the calcined copper-modified cubic mesoporous materials. The molar ratio of zinc and copper acetates in the initial solution is (a) $Zn^{2+}/Cu^{2+} = 4/0$, (c) $Zn^{2+}/Cu^{2+} = 3/1$, and (f) $Zn^{2+}/Cu^{2+} = 2/2$, and (g) 24 wt % Cu-modified on the (a) sample by the wetness impregnation method.

precipitation of copper hydroixde. Possibly, the cupric salt may be coprecipitated together with the cubic mesoporous silica. During the hydrolysis and condensation of silica species, local protons in the reaction solution could be instantly consumed and the pH value thus could be improved in the micro-environment; at the same time, co-deposition of copper species occurred. However, such improved micro-environment is still not suitable for zinc salts to form precipitation under the present circumstances and further studies are needed in the future.

Figure 11 demonstrates the TEM image of the sample synthesized with a molar ratio of $Zn^{2+}/Cu^{2+} = 2/2$. A typical pattern for a material possessing a structure lying on the gyroid infinite periodic minimal surface can be observed, indicating that the symmetry of *Ia*3*d* is maintained even though 24.2 wt % copper has been introduced in the sample by the direct synthesis method. Figure 11 also shows the nitrogen sorption isotherms and pore size distributions of the samples synthesized with different molar ratio of Zn^{2+}/Cu^{2+}. All of the samples containing different amounts of copper possess the sorption isotherms of type IV isotherms with a sharp capillary condensation step indicative of mesopores narrowly distributed in size. Table 2 summarizes the structural and textural properties of the samples prepared with different copper contents. Dispersion of copper species on the cubic silica changes the textural property of resulting samples, and the surface areas of the copper-modified samples synthesized with $Zn^{2+}/Cu^{2+} = 3/1$ and 2/2 are reduced from 712 (without cupric salt) to 523 and 369 m^2/g while the pore volume declined from 1.05 to 0.95 and 0.67 cm^3/g, respectively. It should be pointed out that the micropore areas and volumes are distinctively decreased in the sample synthesized with $Zn^{2+}/Cu^{2+} = 3/1$, where only 0.86 wt % copper species has been loaded. This phenomenon implies that the introduced copper species possibly first enter the micropores of the OMMs and then fill the mesopores of the cubic sample because the main pore diameter of the sample synthesized with $Zn^{2+}/Cu^{2+} = 3/1$ (9.2 nm) is not changed but that of the sample with $Zn^{2+}/Cu^{2+} = 2/2$ (7.6 nm) is distinctively lowered. A traditional wetness impregnation method is also used to modify the cubic OMMs with copper oxides to compare with the direct modification. Much lower surface area and pore volume are detected on the sample prepared by impregnation; nonetheless, the main pore size is not changed, indicating the different deposition mechanisms in impregnation and direct synthesis methods. In general, direct synthesized sample often shows the textural property superior to that of the sample prepared by impregnation because it omits one hydrothermal treatment step and one calcination process, similar to that in the metal-modified SBA-15,[46,47] preventing the shrinkage of silica wall.

UV-DRS, XPS, FTIR, and ICP techniques are employed to explore the dispersion and the state of copper in the copper-containing composites. Figure 12A gives the UV-DR spectra of the resulting samples. Mesoporous silica shows an absorption band around 350−270−204 nm, similar to that

(46) Wei, Y. L.; Wang, Y. M.; Zhu, J. H.; Wu, Z. Y. *Adv. Mater.* **2003**, *15*, 1943.
(47) Wang, Y. M.; Wu, Z. Y.; Wei, Y. L.; Zhu, J. H. *Microporous Mesoporous Mater.* **2005**, *84*, 127.

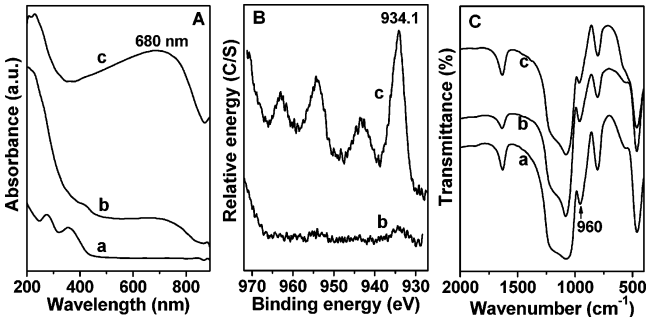

Figure 12. UV-DRS (A), XPS (B), and FTIR (C) results of the copper-modified cubic mesoporous materials with addition of different zinc and copper acetates in original solutions: (a) $Zn^{2+}/Cu^{2+} = 4/0$, (b) $Zn^{2+}/Cu^{2+} = 3/1$, and (c) $Zn^{2+}/Cu^{2+} = 2/2$.

of siliceous MCM-41[48] and attributed to the characteristic of silica.[49] When the cubic material is modified with 0.86 wt % copper, two asymmetric bands appear near 250−280 and 600−850 nm, due to the $Cu^{2+} \leftarrow O^{2-}$ charge-transfer transitions[50] and d−d transitions of dispersed Cu^{2+} species ($3d^9$).[51] As expected, the low intensity of d−d bands is observed on the sample synthesized with $Zn^{2+}/Cu^{2+} = 3/1$ while a strong intensity emerges in the sample prepared with $Zn^{2+}/Cu^{2+} = 2/2$. Besides, these observed d−d transitions situate in the range expected for Cu^{2+} species in an axially distorted octahedral environment of O-containing ligands,[51] and there is no band assigned to metallic or monovalent copper in the spectrum. The transition at 680 nm, which indicates bulk CuO, obviously emerges in the sample synthesized with $Zn^{2+}/Cu^{2+} = 2/2$, which is in accordance with the results of wide-angle XRD. Figure 12B gives XPS results of the copper-modified samples. The binding energy (BE) of Cu $2p_{3/2}$ is 934.4 and 934.1 eV in the sample synthesized with $Zn^{2+}/Cu^{2+} = 3/1$ and 2/2, respectively, which is characteristic of Cu^{2+} within the experimental error[51] but different from that of bulk CuO (933.7 eV). Such a shift of Cu $2p_{3/2}$ peak toward high energy in the copper-modified mesoporous silica results from the dispersion and the interactions between copper oxide moieties and silica support.[52] No band is observed around 936.1 eV, which indicates the absence of Cu−O−Si−O.[51] FTIR spectra give a clue to qualitatively detect the interactions between copper and silica. The 960 cm^{-1} band declines on the sample synthesized with $Zn^{2+}/Cu^{2+} = 2/2$ but unchangeable on the one with $Zn^{2+}/Cu^{2+} = 3/1$ (Figure 12C), mirroring the interactions between the surface silanols and Cu species in the sample with high copper content.[39] According to the ICP analysis, little copper is exchangeable in the sample synthesized with $Zn^{2+}/Cu^{2+} = 2/2$. After the as-prepared sample is ion-exchanged by sodium chloride, about only 0.1 wt % of sodium can be detected while the copper content remains unchangeable. When the sample is calcined at 773 K to convert copper salt to CuO and then thoroughly eluviated by HCl solution, about 1.3 wt % copper remains, which confirms the FTIR result that there is some copper species that interacted with silanols. Nevertheless, this residual copper seems to not be trapped in the pore wall, forming Cu−O−Si−O structure because of the absence of the 936.1 eV peak in the XPS spectrum. On the basis of the UV-DRS, XPS, FTIR, and ICP results, it is conclusive, at least tentatively, that most of the copper species are dispersed in the cubic silica in the form of CuO and a few copper species have a relatively weak interaction with the siliceous support.

Other metal salts such as aluminum, nickel, and ferric salts are also tried to be introduced into the cubic mesoporous material together with zinc acetate, and among them only ferric species can be successfully loaded on the cubic material. Figure S4 indicates the XRD patterns of the as-prepared ferric-modified sample with addition of zinc acetate and ferric chloride in the initial solution. The molar ratio of the reaction mixture is $Zn(CH_3COO)_2/FeCl_3/HCl/TEOS = 3.5/0.5/4.5/1$. The symmetry of *Ia3d* remains in the sample and the ferric species is deposited as hydroxide of FeO(OH), similar to that in the ferric-modified MCM-48 sample by impregnation method.[53] However, the synthetic range of the ferric-modified sample is narrower than that of copper-modified analogues. Either enhancing the molar amount of ferric species or changing the amount of HCl will lead to less ordered mesostructure of the resulting sample. Meanwhile, the weak solubility of ferric hydroxide makes the modified content imprecise like that in copper-modified samples. The amount of the water used in the washing process will affect the deposited ferric content because part of the ferric species can be removed, which is different from that of copper-modified sample where it is difficult to wash off the co-deposited Cu(OH)Cl precipitation so that the copper content is constant once the molar ratio of the reaction mixture is fixed. The reason why copper acetate precursor can play the proper role in the direct synthesis process may be the appropriate solubility product constant (K_{sp}) of copper hydroxide and further investigation is also requested for a deep understanding of these phenomena.

NO_2-TPD experiment is performed to examine the adsorptive capability of the cubic materials. Table 2 lists the NO_2-TPD data of the cubic *Ia3d* sample and its copper-modified analogues. About 53 μmol/g of NO_2 releases from the siliceous material while 100 μmol/g is detected on the sample consisting of 0.86 wt % copper species. When the copper content increases to 24.2 wt %, 506 μmol/g of NO_2 desorbs from the copper-modified material during the test process, indicating an excellent NO_2 capturer derived from the cubic mesoporous material containing copper species. Copper-containing zeolites are the very famous materials for selective adsorption and reduction of NOx in the field of environment catalysis,[51,54] and incorporation of copper can dramatically accelerate the adsorption of NO_2 in SBA-15.[55] Our investigation confirms the high performance of copper-

(48) Wu, Z. Y.; Wang, Y. M.; Zhu, J. H. *Stud. Surf. Sci. Catal.* **2005**, *156*, 139.
(49) Weckhuysen, B. M.; Schoonheydt, R. A. *Catal. Today* **1999**, *49*, 441.
(50) Praliaud, H.; Mikhailenko, S.; Chajar, Z.; Primet, M. *Appl. Catal., B* **1998**, *16*, 359.
(51) Bennici, S.; Gervasini, A.; Ravasio, N.; Zaccheria, F. *J. Phys. Chem. B* **2003**, *107*, 5168.
(52) Espinos, J. P.; Morales, J.; Barranco, A.; Caballero, A.; Holgado, J. P.; Gonzalez-Elipe, A. R. *J. Phys. Chem. B* **2002**, *106*, 6921.
(53) Dapurkar, S. E.; Badamali, S. K.; Selvam, P. *Catal. Today* **2001**, *68*, 63.
(54) Yahiro, H.; Iwamoto, M. *Appl. Catal., A* **2001**, *222*, 163.
(55) Zhou, C. F.; Wang, Y. M.; Cao, Y.; Zhuang, T. T.; Huang, W.; Chun, Y.; Zhu, J. H. *J. Mater. Chem.* **2006**, *16*, 1520.

Table 3. pH Values of the Molar Compositions of Zinc-to-Acid Which Lead to Cubic *Ia*3*d* Mesostructure

$Zn(CH_3COO)_2$/HCl	2/4	2/4.5	2.5/6	3/5	3/6	3/6.5	4/6	4/7	4/8	5/7
pH value	1.94	0.72	0.42	2.92	2.08	0.81	3.07	2.62	2.04	2.92

modified mesoporous materials. The desorbed amount of nitrogen oxides on the sample synthesized with $Zn^{2+}/Cu^{2+} = 2/2$ is enhanced about 9 times larger than that on the parent siliceous sample. Further, the desorption peaks of nitrogen oxides suspend to higher temperature once copper is dispersed on the cubic material. The desorption peak on the siliceous sample is at about 413 K, while those of the samples containing 0.86 and 24.2 wt % copper are at 493 and 553 K, respectively (Figure 9). This is due to the fact that the CuO species can strongly capture the NO_2 in TPD experiment[55] so that the higher desorption temperature is observed in the copper-modified samples, which is beneficial for design and preparation of new functional materials to protect the environment.

Discussion

Synthesis of the siliceous and the in situ copper-modified cubic *Ia*3*d* mesoporous silica is based on the use of metal salt additives in the weak acidic aqueous solution containing Pluronic P123, providing an easier way to obtain cubic phases above pH = 2, the isoelectric point. Three factors, salt, acid, and the inorganic precursor (TEOS), affect the formation of cubic sample with *Ia*3*d* symmetry, and among them acetates additive is crucial because no cubic structure forms if only the acidity of synthetic solution is adjusted without adding acetates. Acetates additives tailor the acidity of the solution containing HCl and P123 and promote the mesostructure transformation from hexagonal to cubic, similar to a function of pH for which Henry and co-worker[56] and Livage, Sanchez, and co-workers[57] developed a simple model to calculate the partial charge held by metal complexes. In our experiment, the effect of acetate additive emerges when the zinc acetate with $x = 1$ is added to the reaction mixture ($x/y/1$ $Zn(CH_3COO)_2$/HCl/TEOS), and thus ordered hexagonal structure can be gained; even the molar of HCl is lowered to $y = 1$ accompanied by a pH value of 4.08. Here the additive seems to delicately adjust the acidity of this batch. However, there is a threshold of the additive amount to affect phase transformation. Under the threshold the additive is helpful in forming ordered hexagonal structure in a wide range of HCl but cannot cause the phase change to cubic. Once the threshold is achieved, acetate additives exert their vital influence in synthesis, and the cubic structure of *Ia*3*d* symmetry appears in the batch with the composition of $2/y/1$ $Zn(CH_3COO)_2$/HCl/TEOS. Further, highly ordered cubic samples are synthesized when the amount of zinc acetate reaches $x = 3$ and 4, and the effect of salt additives will be discussed in detail later.

Acetate additive is not the exclusive factor in controlling the phase transformation. Acidity, concretely, $[H^+]$, in the reaction mixture is also crucial because it can make contributions to the dissolution of reagents, hydrolysis, and condensation of silicate precursors and thus affect the structure evolution.[58] Different possible interactions will take place at the inorganic-template hybrid interface with different pH value.[59] At low acid concentration (pH above 2.7), disordered mesostructures are obtained when using TEOS as the silica source because the hydrolysis rate can compete with the rate of condensation.[60] Using either TMOS (tetramethoxysilane) in the presence of fluoride[61] or the method of pre-hydrolyzation of TEOS[62,63] can widen the synthesis range, where the pH value of the synthetic system can be above the isoelectric point of silica (pH = 2). In our experiments, when acetates were added to the solution containing HCl and P123, the pH value of the mixture would be changed according to the amounts of acetates and HCl and their molar ratio. Table 3 lists the pH values of the compositions that lead to cubic *Ia*3*d* mesostructures along with different molar ratios of $x/y/1$ $Zn(CH_3COO)_2$/HCl/TEOS. It is evident that the cubic mesostructures are formed over a pH range from 0.4 to 3.1, the majority of which is around the isoelectric point of silica (pH = 2). Both hydrolysis and condensation rate of the silica species are pH-dependent. At the pH values lower than the isoelectric point, the condensation becomes faster as the pH decreases. When the pH value exceeds 2, the condensation rate increases until the pH value achieves 8 and then decreases again.[64] The lower concentrations of the acid catalyst provide more flexibility and facilitate the synthesis of large-pore mesoporous silica in more designed ways.[21c] Hence, in the synthesis around pH of about 2, the condensation rate of the silica species is lower than that at strong acidic conditions. And so, phase transformation easily occurs around pH = 2.

The amount of TEOS in the initial reaction solution is also vital for the formation of cubic structure. Adding more silica source (TEOS) in the synthesis of SBA-15 leads to thicker framework walls,[26a] resulting in the plugged hexagonaol templated silica with more micropores along with a higher thermal, hydrothermal, and mechanical stability than traditional SBA-15.[65] In the synthesis using BuOH as cosolute, the phase region for the gyroid *Ia*3*d* structure is well-defined in a wide range of TEOS and thus an approximately linear relationship between the amounts of BuOH and TEOS is observed.[21c] However, in our case, cubic samples with *Ia*3*d* symmetry only form in a very narrow range of TEOS concentrations. Say, highly ordered cubic mesostructure forms at $z = 0.8$ or 1.0 with suitable zinc and acid concentrations, i.e., in the batches of $4/6/z$ $Zn(CH_3$-

(56) Alam, T. M.; Henry, M. *Phys. Chem. Chem. Phys.* **2000**, *2*, 23.
(57) Miled, O. B.; Boissiere, C.; Sanchez, C.; Livage, J. *J. Phys. Chem. Solids* **2006**, *67*, 1775.
(58) Brinker, C. J. *J. Non-Cryst. Solids* **1998**, *100*, 31.
(59) Soler-Illia, G. J. de A. A.; Crepaldi, E. L.; Grosso, D.; Sanchez, C. *Curr. Opin. Colloid Interface Sci.* **2003**, *8*, 109.
(60) Schmidt-Winkel, P.; Yang, P.; Margolese, D. I.; Chmelka, B. F.; Stucky, G. D. *Adv. Mater.* **1999**, *11*, 303.
(61) Kim, J. M.; Han, Y.-J.; Chmelka, B. F.; Stucky, G. D. *Chem. Commun.* **2000**, 2437.
(62) Boissière, C.; Larbot, A.; van der Lee, A.; Kooyman, P. J.; Prouzet, E. *Chem. Mater.* **2000**, *12*, 2902.
(63) Cui, X.; Zin, W.-C.; Cho, W.-J.; Ha, C.-S. *Mater. Lett.* **2005**, *59*, 2257.
(64) Lin, H. P.; Mou, C. Y. *Acc. Chem. Res.* **2002**, *35*, 927.
(65) Van Der Voort, P.; Ravikovitch, P. I.; De Jong, K. P.; Neimark, A. V.; Janssen, A. H.; Benjelloun, M.; Van Bavel, E.; Cool, P.; Weckhuysen, B. M.; Vansant, E. F. *Chem. Commun.* **2002**, 1010.

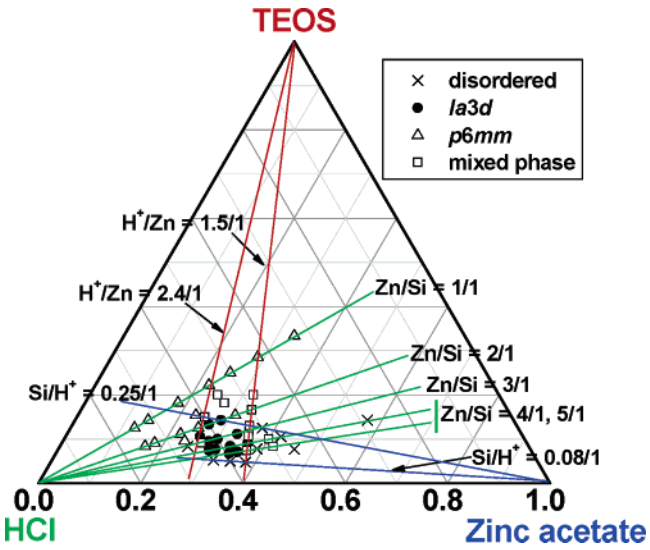

Figure 13. Ternary phase diagram of the structures obtained in the system by adding zinc acetate into the solution containing P123 and HCl. The molar composition of the mixtures is *x*/*y*/*z*/0.017/192 $Zn(CH_3COO)_2$/HCl/TEOS/P123/H_2O.

$COO)_2$/HCl/TEOS, cubic sample emerges only at $z = 1$. Lower concentration ($z < 1.0$) may fail to provide enough inorganic precursors interacting with micellar surfaces, leading to disordered structure; hence, no mesophase can be gained at $z = 0.5$ no matter how the molar compositions of zinc and acid are tuned. Contrarily, higher concentration of TEOS leads to fast condensation and then hinders the phase transformation so that pseudo-cubic *Ia*3*d* or less ordered structure forms once *z* reaches 1.2 or more (4/6/*z* $Zn(CH_3COO)_2$/HCl/TEOS). Occasionally the heightened amount of HCl can exhibit a compensation for the concentration of TEOS through accelerating hydrolysis and condensation of the inorganic precursors. Once *z* rises to 0.8, the molar proportion of HCl increases to $y = 6.5$ or 7.0; cubic samples appear at high zinc concentration (4/*y*/*z* $Zn(CH_3COO)_2$/HCl/TEOS) but are absent at $y = 5.5$ and 6.0. To gain the cubic structure, it is necessary to tune the rate of silica hydrolysis/condensation and the co-assembly rate of silica and polymer during the synthesis. Therefore, the amount of inorganic precursors (TEOS) should be carefully controlled in the initial chemical compositions.

In general, a triangular phase diagram is used to show the importance of chemical composition of an incipient reaction system for structure formation in synthesis.[66,67] Figure 13 depicts the triangular phase diagram to map the range of cubic mesophase in the SiO_2−P123−$ZnAc_2$−H_2O−HCl system (here, $ZnAc_2$ represents zinc acetate). Cubic structure with *Ia*3*d* symmetry forms only in a strictly limited range of TEOS molar ratios, from 0.07 to 0.14 mol %. Lower ratio will result in disordered phase while higher ratio leads to mixed and *p*6*mm* structures. The favorable range of molar ratio of $ZnAc_2$ in the ternary phase diagram is wider, from 0.27 to 0.36 mol %. Structure of *p*6*mm* symmetry establishes at Zn/Si = 1/1 while cubic *Ia*3*d* forms at Zn/Si = 2/1 though the phase range is still narrow. Elevating the Zn/Si value to 3/1 and 4/1 can considerably extend the phase range but further increment to Zn/Si = 5/1 narrows the phase range of *Ia*3*d* structure whereas the less ordered mesophase widely presents in the diagram when Zn/Si > 5/1. The favorable range of HCl concentration is also wider than that of TEOS in the tricomposition system; cubic phase can be assembled in the range of 0.55−0.63 mol %, while ordered hexagonal structures are constructed at either higher or lower concentration of HCl with the assistance of zinc acetate. For example, *p*6*mm* structure is easily obtained with a molar ratio of H^+/Zn above 2.4/1 while less ordered phase appears at the H^+/Zn below 1.5/1 (Figure 13) and cubic phase can be synthesized in the H^+/Zn ranges from 2.4/1 to 1.5/1. Based on these results, the optimum composition for synthesis of cubic material in this system seems to be 0.33−0.36/0.55−0.60/0.09−0.11 mol % for $ZnAc_2$/HCl/TEOS. As mentioned before, similar composition for synthesis of cubic *Ia*3*d* structure is observed in the system by adding cupric, calcium, magnesium acetate, and magnesium nitrate (Figure 7), though the reaction temperature for these systems are different due to different salt effects.

For the synthesis of nonionic copolymer-templated mesoporous materials, many parameters such as the composition and temperature will determine the final mesostructure. In our syntheses, $[H^+]$ can be simply adjusted by changing the amount of HCl and the different salts added into the solution. Cubic *Ia*3*d* mesoporous silica can be attained not only under strong acidic conditions (with $[H^+] > 1$ M) but also above the isoelectric point of silica (pH = 2). Only $Mg(CH_3COO)_2$ and $Ca(CH_3COO)_2$ can lead to cubic *Ia*3*d* mesoporous silica at 288 K while much less ordered mesoporous materials are obtained from other salts (figure not shown). However, other salts are capable of forming cubic silicas at higher temperature, as demonstrated in Table 1. Because the almost same pH values in the mixtures from $Mg(CH_3COO)_2$ and $Cu(CH_3COO)_2$ and the very close pH values in those from $Ca(CH_3COO)_2$ and $Zn(CH_3COO)_2$ lead to quite different mesostructures under otherwise same conditions, $[H^+]$ should not be the single determining role in the formation of cubic *Ia*3*d* mesoporous silica. Hereby, the reason why different synthetic temperatures are desirable for the mixtures with specific salt can be tentatively explained by the Hofmeister effect.

According to the Hofmeister sequence of cations (NH^{4+} > K^+ > Na^+ > Cs^+ > Li^+ > Mg^{2+} > Ca^{2+} > Cu^{2+} > Cd^{2+} > Zn^{2+} > Ce^{3+}),[68−70] Mg^{2+} belongs to salting-in ions that are large and have large polarizabilities; thus, they are certainly expected to hydrate the nonionic micellar surfaces and to raise the surfactant cloud point, leading to slower precipitation of the surfactant−silica composite.[68] In the case of the synthesis with $Mg(CH_3COO)_2$/TEOS = 3 at 288 K, silica−polymer composite precipitates about 12 h after the addition of TEOS. The much slower condensation provides a flexible network in favor of mesophase transformation and

(66) Grosso, D.; Cagnol, F.; Soler-Illia, G. J. A. A.; Crepaldi, E. L.; Amenitsch, H.; Brunet-Bruneau, A.; Bourgeois, A.; Sanchez, C. *Adv. Funct. Mater.* **2004**, *14*, 309.
(67) Doshi, D. A.; Gibaud, A.; Goletto, V.; Lu, M.; Gerung, H.; Ocko, B.; Han, S. M.; Brinker, C. J. *J. Am. Chem. Soc.* **2003**, *125*, 11646.
(68) Leontidis, E. *Curr. Opin. Colloid Interface Sci.* **2002**, *7*, 81.
(69) Cook, H. A.; Dicinoski, G. W.; Haddad, P. R. *J. Chromatogr. A* **2003**, *997*, 13.
(70) Keast, R. S. J.; Breslin, P. A. S. *Pharm. Res.* **2002**, *19*, 1019.

so a new cubic *Ia*3*d* mesostructure can be formed.[21c,71,72] Ca^{2+} has the salting-in effect similar to that of Mg^{2+}; thus, under almost the same conditions calcium acetate facilitates the formation of cubic *Ia*3*d* mesostructure. Cu^{2+} and Zn^{2+} have stronger salting-in effect than that of Mg^{2+}, leading to the much slower precipitation and thus the poorly ordered mesostructure at 288 K (Figure S5A). However, raising the synthetic temperature up to 308 K can accelerate the rate of precipitation to make up for too strong salting-in effect of Cu^{2+} and Zn^{2+}. Thus, cubic *Ia*3*d* mesoporous silicas can be obtained with $Zn(CH_3COO)_2/HCl = 3/6$ or $Cu(CH_3COO)_2/HCl = 3/6$ at 308 K. In the case of $Mg(NO_3)_2$, both Mg^{2+} and NO^{3-} are salting-in ions; accordingly, the desirable synthetic temperature is higher, 313 K, to accelerate the silica condensation and the co-assembly of silica and polymer. In contrast, when potassium acetate is used with the same acetate concentration, no mesostructure is obtained, which may contribute to the salting-out effect of both K^+ and CH_3COO^-, leading to faster precipitation and thereby the absence of ordered mesostructure. All these data prove that bivalent cations with salting-in effect can control the precipitation rate of the silica−polymer composite in favor of the formation of cubic *Ia*3*d* mesoporous silicas.

On the other hand, anion in the salts also affects the mesostructure.[73] With use of magnesium sulfate, chloride, and nitrate instead of acetate with otherwise same conditions at 288 K, the 2D hexagonal *p*6*mm* mesostructure is obtained in the case of using sulfate, while poorly ordered mesophases are observed in the cases of chloride and nitrate (Figure S5B). The aggregation number or ionic radii are decreased in the following order: $^1/_2SO_4^{2-} > Cl^- > NO_3^-$;[15] Hofmeister effect of anions follows the sequence: $SO_4^{2-} > CH_3COO^- > Cl^- > NO_3^-$.[68] Hence, the strong salting-out effect of SO_4^{2-} predominates the salting-in effect of Mg^{2+}, similar to the situations in the presence of KCl where both K^+ and Cl^- show salting-out effect and then lead to a *p*6*mm* mesostructure. In the cases of magnesium chloride and nitrate, the salting-out effect of Cl^- is rather weak and NO_3^- behaves like the salting-in effect; thus, the salting-in effect dominates the syntheses, where the hydrolysis and condensation of silica species are too slow to form highly ordered mesostructure. In the case of magnesium acetate, the salting-in effect of Mg^{2+} is delicately balanced by the salting-out effect of CH_3COO^-, which not only ensures the formation of highly ordered mesostructure at low temperature but also achieves the flexible silica network to form a new cubic *Ia*3*d* mesophase. It should be pointed out that the salt effect caused by the ions is not the only factor to decide the structure. Temperature, pH value, chemical composition, and so on are all vital in the formation of cubic *Ia*3*d* mesostructures in our experiments, as aforementioned.

Cubic structures can be synthesized in a wide pH range by adding bivalent salts into the solution containing P123 and HCl, however, whose mechanism is somewhat different from that of $SiO_2-P123-BuOH-H_2O-HCl$ or $SiO_2-P123-NaI-H_2O-HCl$ system. For the system using BuOH, formation of mesophase is mainly governed thermodynamically and lamellar phase appears in the initial step and then transforms to cubic phase.[21c] In the system containing NaI salt, phase segregation has happened before introduction of TEOS and precipitation starts almost directly after the TEOS addition. So the addition of NaI salt may affect the kinetic variations and then cause the structural changes.[10] However, two fundamental aspects, thermodynamic and kinetic, coexist in phase formation and/or transformation. In our case, acetate additive decreases the acidity of reaction mixture and affects the solubility properties of P123 surfactant. Besides, introducing acetate may bring out a more thermodynamically stable system in which salt cooperates with the polymers to induce phase transformation. The possible interaction between micelle and bivalent salt in the $SiO_2-P123-acetate-H_2O-HCl$ system, together with the weak acidity, may affect the hydrolysis and polymerization of the silica species and then cause phase change, which however needs to be studied in detail.

Conclusion

1. Highly ordered mesoporous silica with bicontinuous cubic *Ia*3*d* structure has been successfully synthesized by adding zinc, magnesium, cupric, calcium acetate, and magnesium nitrate into the synthetic solution containing P123 and HCl. Acidity of the solution is tuned by adding zinc acetate, and the cubic mesostructure can be formed in a wide range of starting mixture compositions. It is the first time that the cubic *Ia*3*d* mesostructure can be templated by P123 in the weak acidic conditions with pH value above 2.

2. A phase diagram has been drawn to map the range of the cubic mesophase in the $SiO_2-P123-ZnAc_2-H_2O-HCl$ system. Effect of the chemical compositions (TEOS, HCl, and $ZnAc_2$) has been thoroughly investigated. The introduced acetates in the system have the function of both modulating the acidity of the solution and helping to change the symmetry of silica−P123 mesophase from *p*6*mm* to *Ia*3*d*. These salt additives cooperate with the polymer and then induce the phase change. Both cation and anion in the salts have a distinct influence on the final mesostructure.

3. Copper-modified cubic materials could be directly synthesized by introducing copper and zinc acetate into the solution containing P123 and HCl. With molar composition of $Zn(CH_3COO)_2/Cu(CH_3COO)_2/HCl/TEOS = 2/2/6/1$, about 24 wt % copper can be dispersed onto the cubic mesoporous silica. This directly synthesized sample shows higher surface area and pore volume than the one prepared with the traditionally impregnation. About 506 μmol/g of NO_2 is desorbed from the 24.2 wt % copper-modified material in the NO_2-TPD process, 9 times larger than that from the siliceous sample.

4. Other metal species are tried to be introduced into the cubic mesoporous material. With the molar ratio of the reaction mixture of $Zn(CH_3COO)_2/FeCl_3/HCl/TEOS = 3.5/0.5/4.5/1$, ferric can be incorporated in the cubic material. The synthetic range of the ferric-modified sample is narrower than that of the copper-modified samples.

(71) Gallis, K. W.; Landry, C. C. *Chem. Mater.* **1997**, *9*, 2035.
(72) Landry, C. C.; Tolbert, S. H.; Gallis, K. W.; Monnier, A.; Stucky, G. D.; Norby, P.; Hanson, J. C. *Chem. Mater.* **2001**, *13*, 1600.
(73) Wang, Y. Q.; Wang, Y. J.; Yang, C.-M.; Lu, G. Z.; Schuth, F. *Langmuir* **2006**, *22*, 5491.

Acknowledgment. We would like to thank NSF of China (20673053 and 20373024) and Analysis Center of Nanjing University for their financial support. Dr. Kai Shen in Nanjing University of Aeronautics and Astronautics is acknowledged for the fulfillment of TEM experiments.

Supporting Information Available: Plot of pH values and phase diagram; XRD patterns; low-angle XRD patterns. This material is available free of charge via the Internet at http://pubs.acs.org.

CM0623615